Electronic Supplementary Information (ESI)

A direct conversion of blast furnace slag to mesoporous silica–calcium oxide composite and its application in CO_2 capture

Yasutaka Kuwahara,*[a,b,c] Aiko Hanaki[a] and Hiromi Yamashita*[a,b]

[a] Division of Materials and Manufacturing Science, Graduate School of Engineering, Osaka University, 2-1 Yamada-oka, Suita, Osaka 565-0871, Japan

[b] Unit of Elements Strategy Initiative for Catalysts & Batteries (ESICB), Kyoto University, Katsura, Kyoto 615-8520, Japan

[c] JST, PRESTO, 4-1-8 Honcho, Kawaguchi, Saitama 332-0012, Japan

*E-mail: kuwahara@mat.eng.osaka-u.ac.jp (Y. Kuwahara)
*E-mail: yamashita@mat.eng.osaka-u.ac.jp (H. Yamashita)
Tel: (+81) 6-6879-7460, Fax: (+81) 6-6105-5029

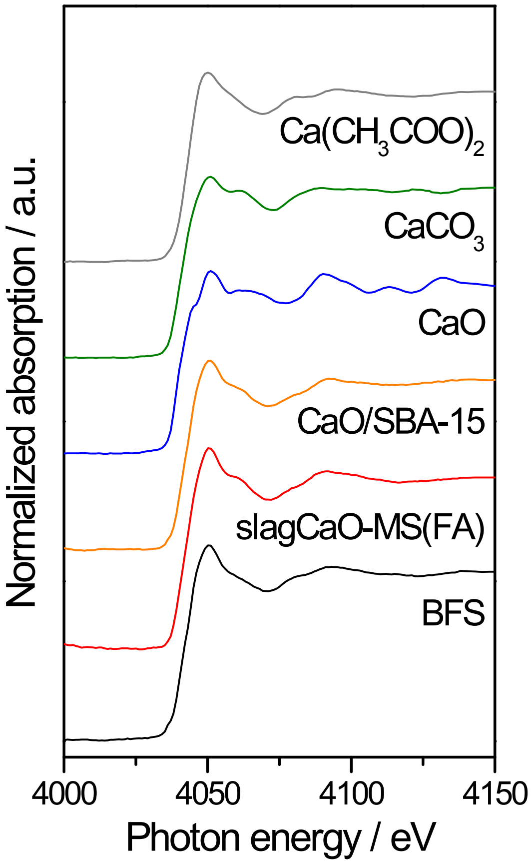

Fig. S1 Ca K-edge X-ray absorption near edge (XANES) spectra of slagCaO-MS(FA), raw BFS and the related Ca-based compounds measured in a fluorescence mode at room temperature.

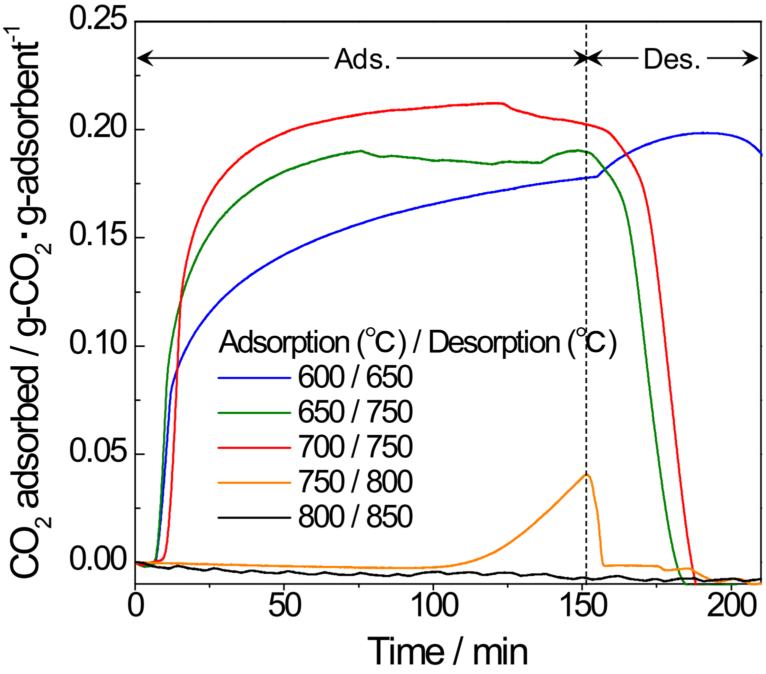

Fig. S2 CO_2 adsorption-desorption testings of slagCaO-MS(FA) measured at different carbonation-decarbonation temperatures. Adsorption: 10% CO_2/N_2 at 600–800 °C for 120 min, Desorption: 100% N_2 at 650–850 °C for 60 min.

Table S1 Summary of CO_2 adsorption-desorption tests of slagCaO-MS(FA) measured at different carbonation-decarbonation temperatures.

Adsorption Temperature (°C)	Desorption Temperature (°C)	CO_2 adsorption capacity (g-CO_2/g)	Remarks
600	650	0.173	CO_2 cannot be desorbed
600	750	0.154	
650	750	0.184	
700	750	0.188	Employed in this study
750	800	0.041	Structure collapsed
800	850	<0.001	Structure collapsed

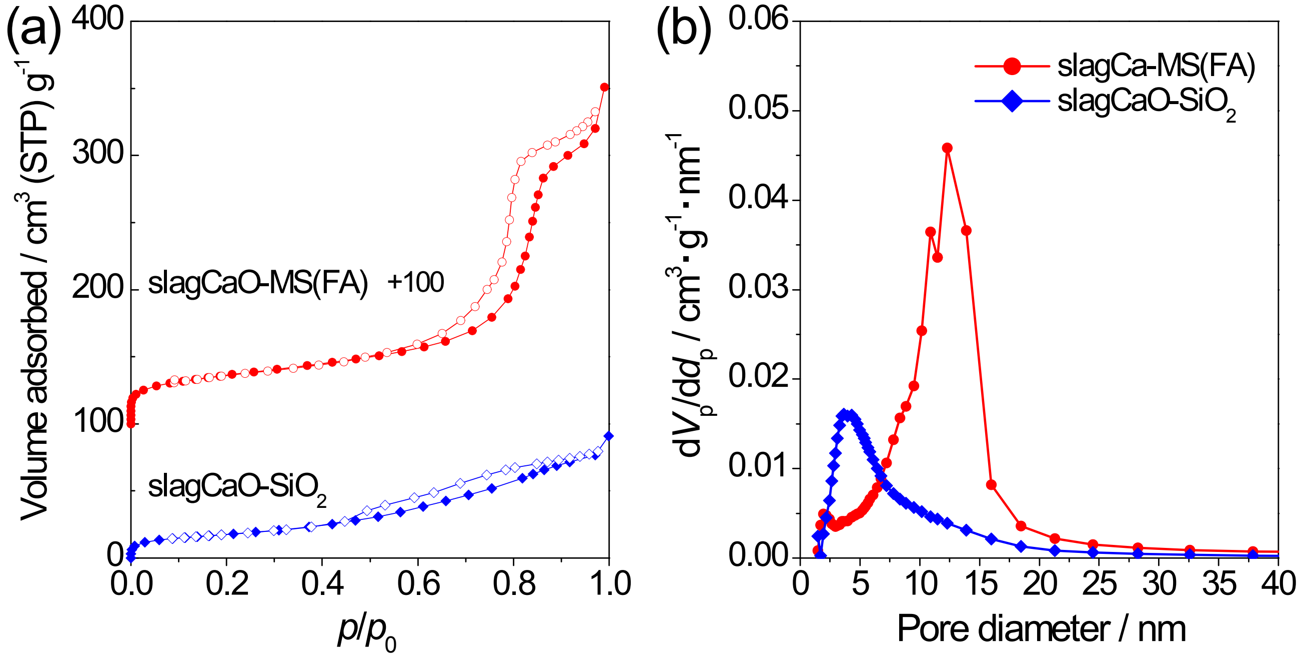

Fig. S3 (a) N_2 adsorption-desorption isotherms and (b) the corresponding BJH pore size distribution curves of slagCaO-MS(FA) and slagCaO-SiO$_2$ (synthesized without P123).

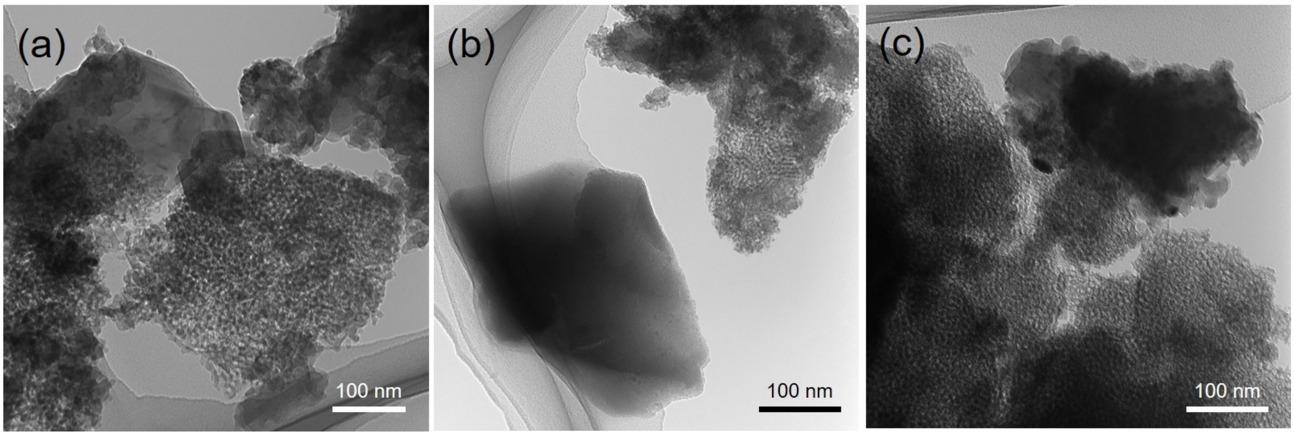

Fig. S4 TEM images of slagCaO-MS(FA) composites synthesized at different hydrothermal temperatures; (a) 100 °C, (b) 130 °C and (c) 150 °C.

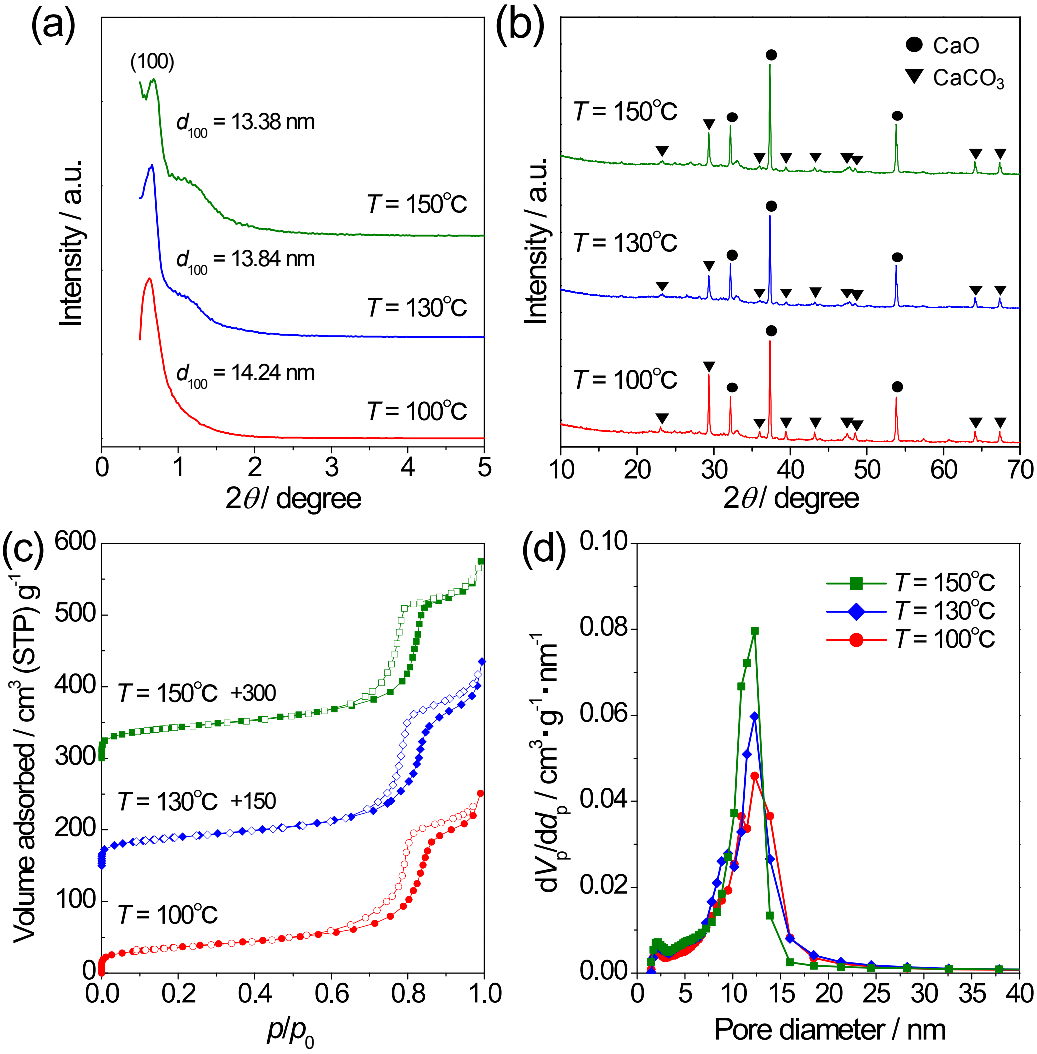

Fig. S5 (a) Low-angle and (b) high-angle XRD patterns, (c) N_2 adsorption-desorption isotherms and (d) the corresponding BJH pore size distribution curves of slagCaO-MS(FA) composite synthesized at different hydrothermal temperatures (*T* = 100, 130 and 150 °C).

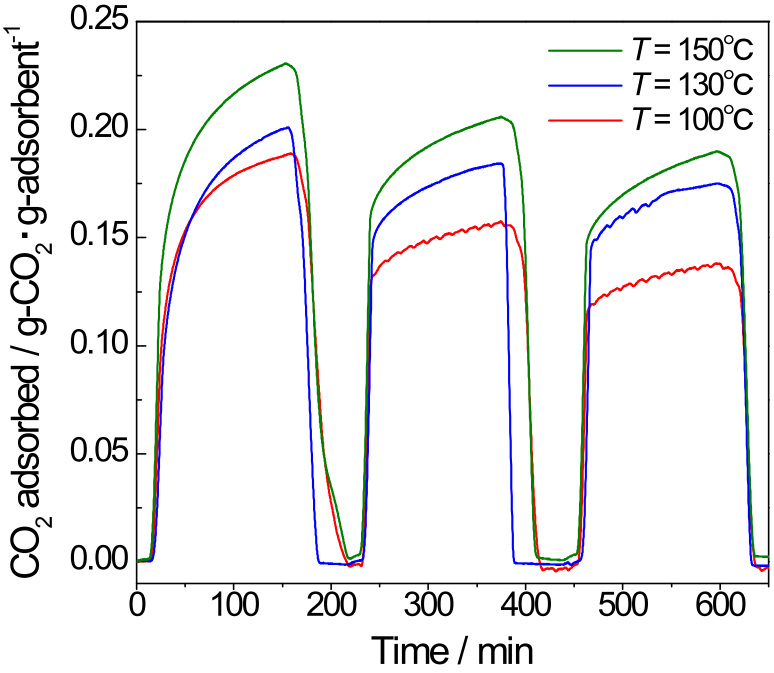

Fig. S6 CO_2 adsorption-desorption testings for 3 repeated cycles of slagCaO-MS(FA) composite synthesized at different hydrothermal temperatures (T = 100, 130 and 150 °C). Adsorption: 10% CO_2/N_2 at 600–800 °C for 120 min, Desorption: 100% N_2 at 650–850 °C for 60 min.

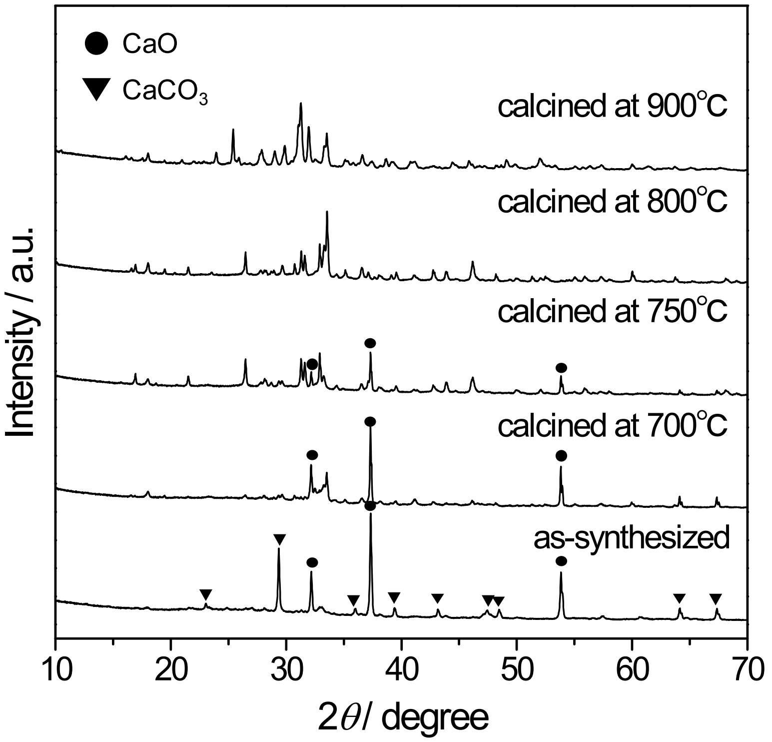

Fig. S7 XRD patterns of as-synthesized slagCaO-MS(FA) and slagCaO-MS(FA) calcined in air at different temperatures (700–900 °C). Unidentified peaks might be attributed to several calciumsilicate crystals.

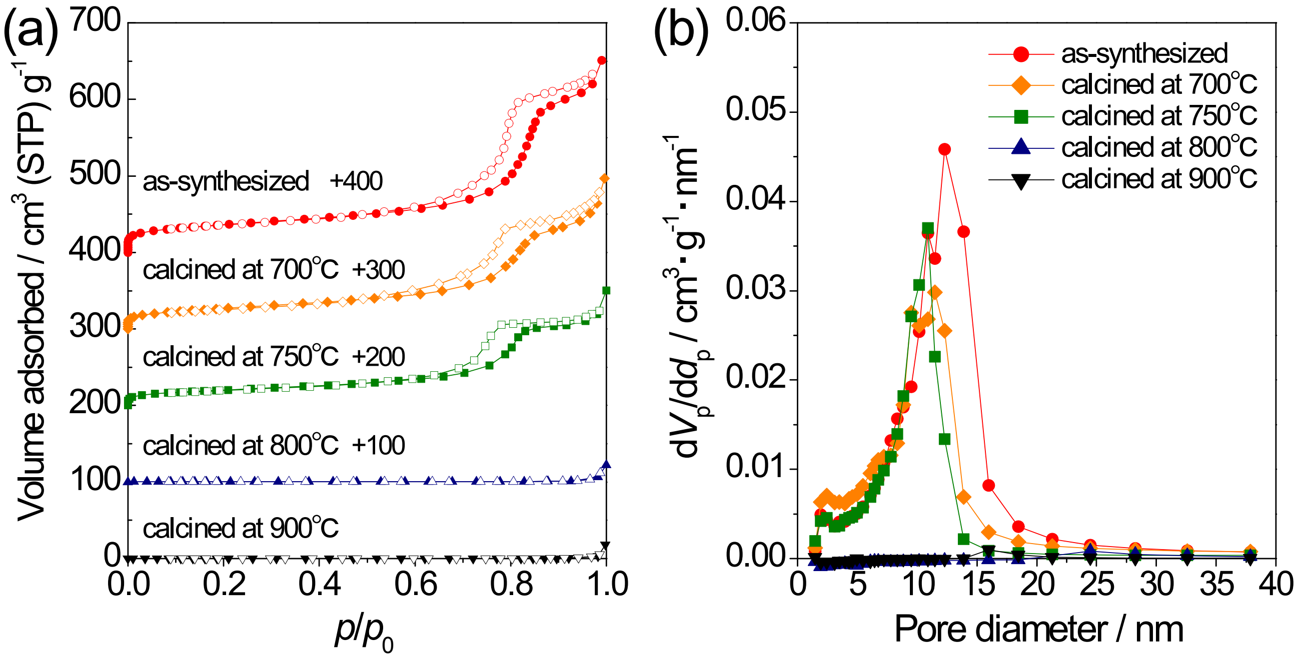

Fig. S8 (a) N_2 adsorption-desorption isotherms and (b) the corresponding BJH pore size distribution curves of as-synthesized slagCaO-MS(FA) and slagCaO-MS(FA) calcined in air at different temperatures (700–900 °C).

Table S2 Textural parameters of as-synthesized slagCaO-MS(FA) and slagCaO-MS(FA) composites calcined in air at different temperatures (700–900 °C).

Calcination Temperature (°C)	S_{BET} [a] $(\mathrm{m^2/g})$	V_{total} [b] $(\mathrm{cm^3/g})$	V_{meso} [c] $(\mathrm{cm^3/g})$	D_{peak} [d] (nm)
As-synthesized (clcined at 600 °C)	128	0.388	0.227	12.3
700	96.5	0.285	0.141	11.5
750	72.9	0.209	0.137	10.9
800	2.1	0.020	-	-
900	1.0	0.016	-	-

[a] Specific surface area calculated by the BET method. [b] Total pore volume reported at p/p_0 = 0.99. [c] Mesopore volume determined from *t*-plot. [d] Peak pore diameter determined by the BJH method.

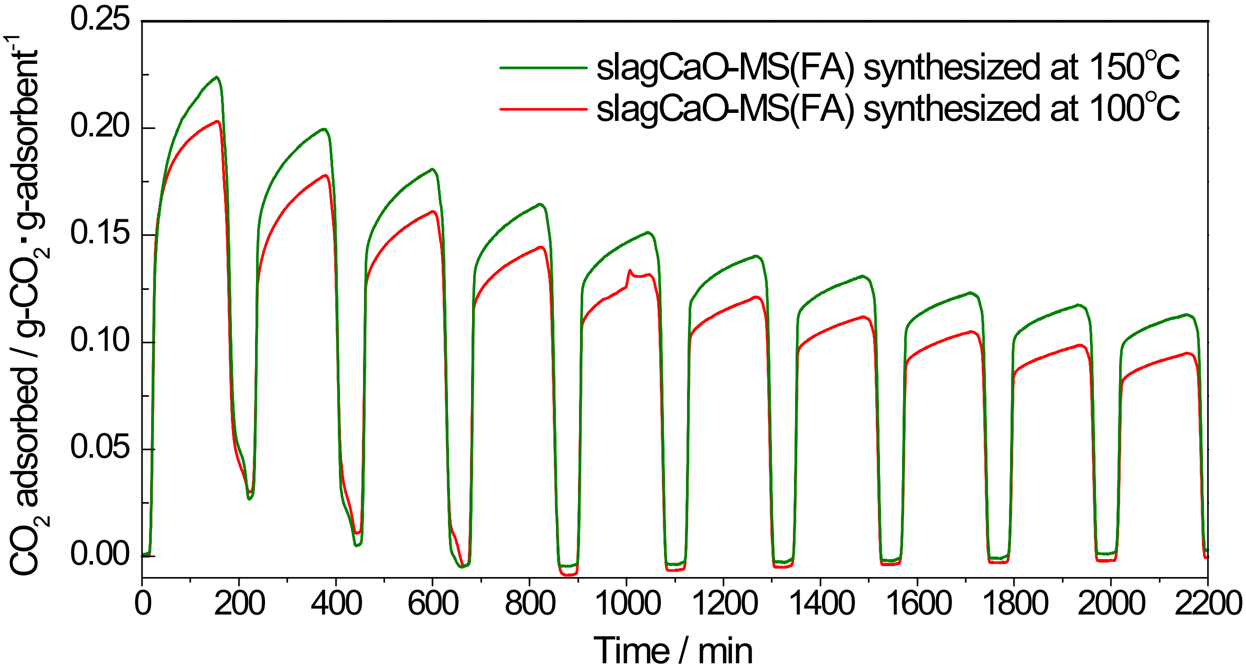

Fig. S9 CO_2 adsorption-desorption testings for 10 repeated cycles of slagCaO-MS(FA) synthesized at 100 and 150 °C. Adsorption: 10% CO_2/N_2 at 700 °C for 150 min, Desorption: 100% N_2 at 750 °C for 60 min.

The Gibbs free energy ($\Delta G^{\circ}{}_{1}$) for the carbonation/decarbonation reaction of calcium oxide

$$\mathrm{CaO(s) + CO_2(g) = CaCO_3(s)} \qquad \text{…(eq.1)}$$

can be expressed as a function of temperature, T, as follows,

$$\Delta G^{\circ}{}_{1} = -\ 178.4\times10^{3} + 160.3\times T\ \mathrm{(J/mol)} \qquad \text{…(eq. 2)}$$

which was determined from the thermodynamic data of each compound shown below,

$$\Delta G^{\circ}(\mathrm{CaO}) = -\ 635.1\times10^{3} - 39.7\times T\ \mathrm{(J/mol)} \qquad \text{…(eq. 3)}$$

$$\Delta G^{\circ}(\mathrm{CO_2}) = -\ 393.5\times10^{3} - 213.6\times T\ \mathrm{(J/mol)} \qquad \text{…(eq. 4)}$$

$$\Delta G^{\circ}(\mathrm{CaCO_3}) = -\ 1207\times10^{3} - 93\times T\ \mathrm{(J/mol)} \qquad \text{…(eq. 5)}$$

The change in Gibbs free energy (ΔG_1) can be expressed as a function of temperature, T, and the equilibrium constant of equation 1, K_1, as follows,

$$\Delta G_1 = \Delta G^{\circ}{}_{1} + RT\cdot \ln K1 = \Delta G^{\circ}1 + RT\cdot \ln(a_{\mathrm{CaCO3}} / (a_{\mathrm{CaO}} \cdot P_{\mathrm{CO2}})) \qquad \text{…(eq. 6)}$$

where R represents the gas constant (8.314 (J/·K·mol)), a_{CaCO3} and a_{CaO} represent the activity of $CaCO_3$ and CaO, respectively, and P_{CO2} represents the partial pressure of CO_2 gas. Given that $CaCO_3$ and CaO are crystallographically pure compounds, equation 6 can be transformed into,

$$\Delta G_1 = -\ 178.4\times10^{3} + 160.3\times T - RT\cdot \ln P_{\mathrm{CO2}} \qquad \text{…(eq. 7)}$$

Thermodynamically considering, the decarbonation reaction of $CaCO_3$ takes place, if $\Delta G_1 > 0$. Therefore, the range of temperature at which the decarbonation reaction of $CaCO_3$ takes place can be expressed as a function of P_{CO2} as follows,

$$T > 178.4\times10^{3} / (160.3 - R\cdot \ln P_{\mathrm{CO2}}) \qquad \text{…(eq. 8)}$$

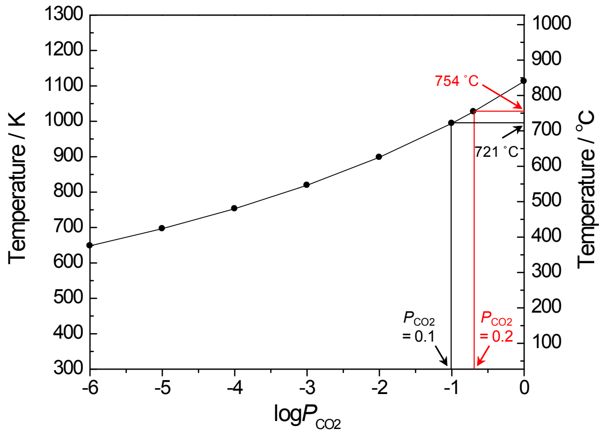

Fig. S10 Theoretical temperature at which decarbonation of $CaCO_3$ takes place plotted on a logarithmic scale of partial pressure of CO_2 (P_{CO2}).

Equation 8 is depicted in Fig. S10, which indicates that the theoretical temperature at which CO_2 is released from $CaCO_3$ under a flow of 10% CO_2 gas stream is about 721 °C. In this study, we performed the CO_2 desorption at 750 °C, which is sufficient to release CO_2 from $CaCO_3$. The theoretical temperature at which CO_2 is released from $CaCO_3$ under a flow of 20% CO_2 gas stream is estimated to be about 754 °C, theoretically showing that capturing/releasing CO_2 from flue gas containing 20% CO_2 is feasible under the temperature conditions employed in this study.